ISSN 2231-3478 (Print)
JUSPS-B Vol. 37(2), 12-19 (2025). Periodicity-Monthly
Section B
(Online) ISSN 2319-8052

JOURNAL OF ULTRA SCIENTIST OF PHYSICAL SCIENCES
An International Open Free Access Peer Reviewed Research Journal of Physical Sciences
website:- www.ultrascientist.org
Estd. 1989

Studies of Absorption and Frequency Upconversion Properties of Erbium ions Co-doped Quaternary Tellurite Glasses

KULDEEP PATEL[1], S.K. MAHAJAN[2], and GHIZAL F. ANSARI[1*]

[1]Physics Department, Madhyanchal Professional University, Bhopal – 462044 MP (India)
[2]Department of Applied Physics, Samrat Ashok Technological Institute,
Vidisha– 464001 MP (India)
*Corresponding Author Email: ansarigf@rediffmail.com, ORCID ID:0000-0002-9278-5436
http://dx.doi.org/10.22147/jusps-B/370201

Acceptance Date 02nd August 2025 **Online Publication Date 11th August 2025**

Abstract

This study investigates the optical absorption and frequency upconversion properties of Erbium (Er^{3+}) ion co-doped quaternary tellurite glasses (TZWE), which have garnered attention due to their promising applications in photonic devices. Tellurite glasses, known for their low phonon energy, high refractive index, and broad transmission window, serve as effective hosts for rare earth ions. The optical band gap energies of the synthesized glasses were determined using Tauc's plot method and found to decrease from 3.14 eV to 3.01 eV with increasing Er^{3+} concentration. Correspondingly, the refractive index increased from 2.36 to 2.39, indicating enhanced polarizability of the glass matrix. UV-Vis-NIR absorption spectra confirmed multiple characteristic transitions of Er^{3+} ions, with intensity rising proportionally to dopant concentration. Upconversion photoluminescence under both 377 nm and 980 nm excitation revealed green and red emissions, primarily attributed to transitions such as $^2H_{11/2} \rightarrow {}^4I_{15/2}$ and $^4F_{9/2} \rightarrow {}^4I_{15/2}$. A detailed energy transfer mechanism, involving ground-state absorption, excited-state absorption, energy transfer upconversion, and cross-relaxation processes, was proposed to explain the luminescent behavior. The results confirm the potential of Er^{3+} -doped tellurite glasses for advanced photonic applications such as lasers and optical amplifiers.

Key words : Erbium-doped tellurite glass; Upconversion luminescence; Optical band gap: Refractive index.

1. Introduction

In the field of photonics researchers have created glasses with different compositions. The oxide compositions that are most frequently investigated are based on borates[1], phosphates[2], and silicates[3]. Although these glasses generally exhibit acceptable mechanical and thermal stabilities, their poor lanthanide dispersion and high melting temperatures prevent them from being used as intended[4]. Glass, a superb homogenized medium with high rare earth solvability, is a key component of photonic materials due to its distinct structural, thermomechanical, and thermodynamical properties[5]. Heavy metal oxide glasses, including those made of antimony, bismuth, germanate, and tellurite, have received particular interest in more recent years. Tellurite glasses in particular provide encouraging qualities such operating at a lower temperature[4]. Excellent tellurite glass has a wide range of uses, including fiber optics, lasers, broadband amplification, optical fiber amplifiers, nonlinear optical devices, and more[7].

In fundamental research and for various photonic applications, erbium-doped tellurite glasses are highly intriguing materials[8-9]. Erbium ion-doped tellurite glasses have been the subject of extensive research globally. Low melting temperature, high refractive index, wide bandwidth, and strong emission cross section at 1.5 nm wavelength are characteristics of erbium-doped tellurite glasses[6,9].

According to the composition, tellurite glass has a higher refractive index than the other (between 1.9 and 2.25)[10,11]. When Er_2O_3 is added to tellurite glasses, the refractive index rises[8]. The strong polarization of the host material TeO_2 is responsible for the high refractive index of tellurite glasses[10,12]. It is know that as the ionic radius of the lanthanide atoms increased, the absorption edge moved to a higher wavelength direction. As the atomic number of rare earth atoms increased, so did the optical energy gap for both direct and indirect prohibited transitions[13-14].

2. Experiment

Melt quenching was used to create quaternary tellurite glass systems in the following forms: $80TeO_2$- 5ZnO-(15-x) WO_3-x Er_2O_3, where x = 0, 0.5, 1, 1.5, and 2 mol%. The batches of extremely pure ingredients were thoroughly mixed and pounded in an agate mortar. The powdered mixture was then heated within an alumina crucible in an air-filled muffle furnace. To reduce the possibility of volatilization, the mixture was kept at 300 °C for 20 to 25 minutes. The batch material determined the temperature, which ranged from 890 to 920 °C. To guarantee that every component melted fully, the melt was left in this range for 30 minutes. To improve homogeneity, it was stirred a few times. Then, at room temperature, the extremely viscous melt was poured into a stainless steel pellet mold with a diameter of 0.8 cm. After that, the sample was kept at 320 °C for 1.2 hours in an annealing furnace. The glass sample was then allowed to cool in the furnace for 10 hours after it was shut off. The produced pellet-shaped samples were referred to as TZWE0, TZWE1, TZWE2, TZWE3, and TZWE4. UV-VIS-IR spectra of synthesized samples were carried by Research India's spectrometer in 200nm to 1100nm range. Upconversoin luminescence study of samples done under the two excitation 377nm and 980nm.

3. Result and Discussion

3.1. Optical Band Gap Energy and Refractive Index

Optical band gap energy is the difference between the valence and conduction bands of glass. We must first convert wavelength into photon energy and then graph absorption spectra in the form of the relationship between the photon energy (hυ) and $(\alpha h\upsilon)^r$ in order to find the optical band gap energy. Tauc's plot methods, which determine the optical gap by extrapolating from the graph to locate the point of intercept to the hυ axis, can be used to determine the optical band gap energy. With α being the absorption coefficient, hυ being the incident photon energy, C being a constant electronic transition, *r* being a type of electronic transition, and Eop being the optical band gap, the optical band gap energy may be calculated using the formula $\acute{a}h\tilde{o} = C(h\tilde{o} - Eop)^r$. For a straight transition, *r* equals ½, whereas for an indirect transition, *r* equals 2. Many oxide glasses, including tellurite, are absorbed by indirect transitions ($r = 2$) [11]. The graph of the (hυ)vs$(\alpha h\upsilon)^{1/2}$ was then made in order to determine the optical band gap energy. The linear extrapolation area $(\alpha h\upsilon)^{1/2}=0$ fits the optical band gap energy value. Figure 1 shows the results of applying Tauc's plot approach to determine the optical band gap energy value.

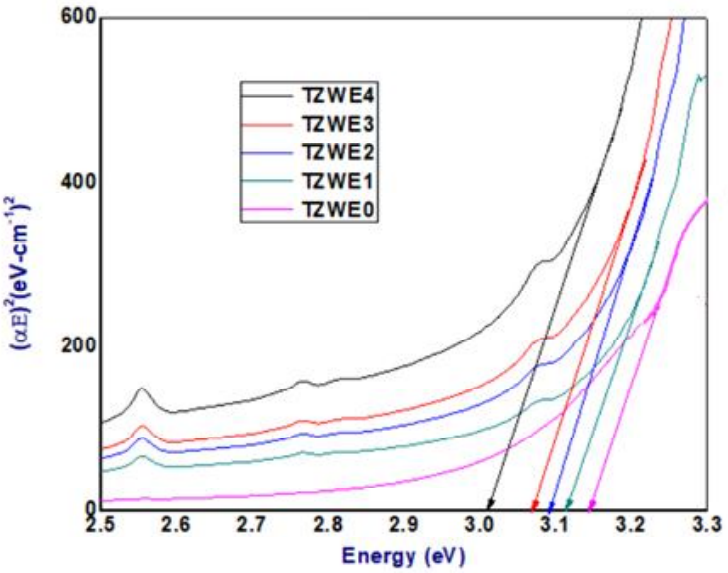

Figure 1 Tauc's plot of TZWE glasses

As the concentration of Erbium ions in TZWE glasses increases, Figure 2 displays the optical band gap energy values that were determined. The optical band gap energy is the value obtained from the linear extrapolation of the $(\alpha h\upsilon)2 = 0$. In samples 1(TZWE0) with x = 0, the optical band gap energy is 3.14 eV; in samples 2(TZWE1) with x = 0.5, it is 3.12 eV and in samples 3 (TZWE2)with x = 1, it is 3.1 eV; in samples 4(TZWE3) with x = 1.5, it is 3.08 eV; in samples 5(TZWE4) with x = 2, it is 3.01 eV.

3.2. Refractive index :

The relationship between the optical energy gap Eop and the refractive index n was investigated by using this relation[15].

$$\frac{n^2-1}{n^2+1}=1-\sqrt{\frac{Eop}{20}} \quad (1)$$

The evaluated values of refractive index of the synthesized glass samples are lies between 2.36 to 2.39, the value of RI increases with increasing Erbium ions concentration.the plot of RI and percentage erbium ions concentration in the TZWE glasses shown in figure 2.

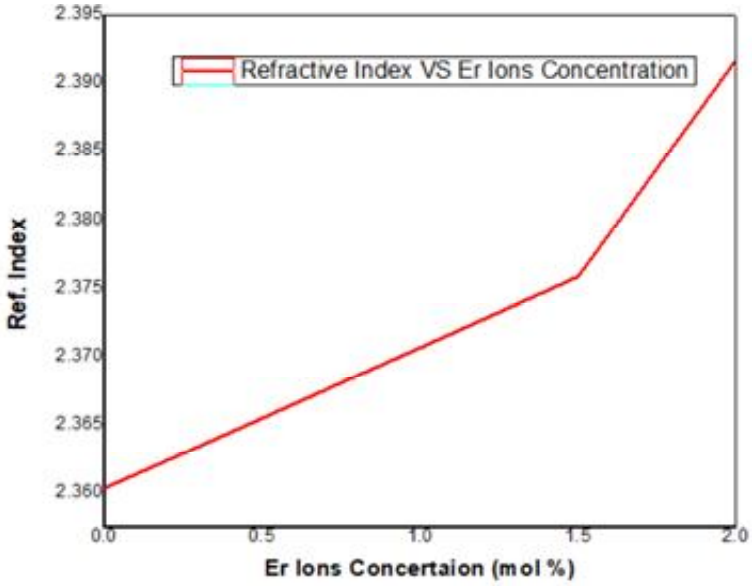

Fig. 2 Refractive Index VS Er Ions Concentration plot

3.3. Absorption Spectra :

Fig 2 shows the UV-Vis-NIR absorption spectra of erbium doped tellurite glasses. The absorption spectra in the range 250- 1100 nm were recorded by a UV- Vis- NIR spectrometer (Make-research India). Based on Fig 2, it can be seen that, the first sample have no peak. It is because of the concentration of Er_2O_3 was 0% mol. Eight peaks are observed in all TZWE glasses. The peaks of these absorption spectra are generated electronics transition from ground state to higher energy states. In general, the greater concentration of Erbium ions in the TZWE glass will be have the greater absorption. Sample 5 with 2% OF Er_2O_3 has the highest optical absorbance than the other samples. The absorption peaks are located at 381, 408, 446, 455, 492, 528, 548, 656, 805, and 980 nm, which are attributed to the transitions from the ground $^4I_{15/2}$ level to $^4G_{11/2}$, $^2H_{9/2}$, $^4F_{3/2}$, $^4F_{5/2}$, $^4F_{7/2}$, $^2H_{11/2}$, $^4S_{3/2}$, $^4F_{9/2}$, $^4I_{9/2}$, and $^4I_{11/2}$ excited states of Erbium ions, respectively.

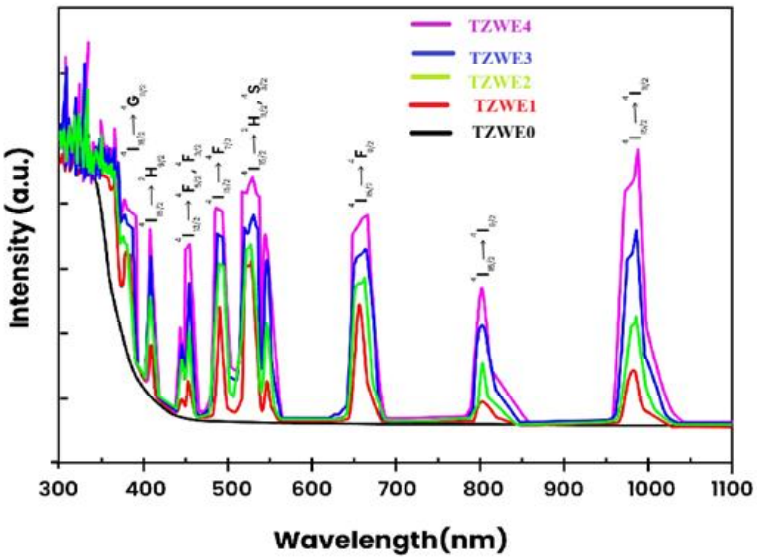

Fig. 2. shows the UV-Vis-NIR absorption spectra of TZWE glasses

3.4. Upconversion Photo-luminescence Under 377 nm Excitation :

A change in Upconversion photo-luminescence of TZWE glaases with Er_2O_3 under 377nm excitation in the 450–750 nm region is shown in Fig. 3. The transitions of $^4I_{15/2} \rightarrow {}^2H_{11/2}$ (521 nm), $^4S_{3/2}$ (543 nm), and $^4F_{9/2}$ (663 nm) of Erbium ions are responsible for the weak red band at 662 nm and the strong green emission band with two peaks at 542 nm and 552 nm [16]. These TZWE glasses also show weak green emission with two peaks at 520 nm and 530 nm. When stimulated at 377 nm, the spectra showed a rise in photo-luminescence output as the Er_2O_3 content in the visible region increased[17].

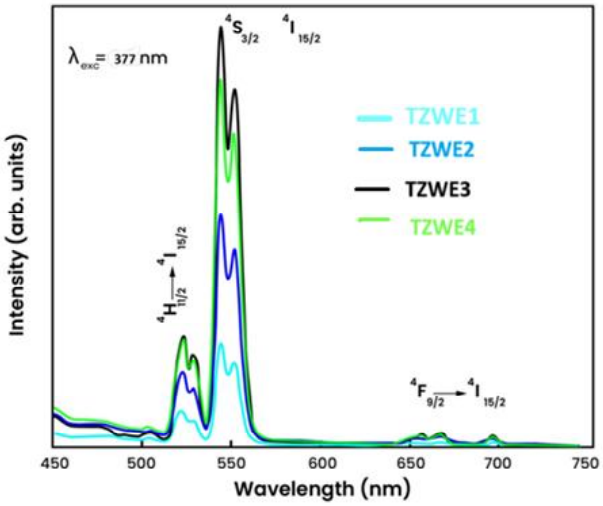

Fig. 3, TZWE glaases with Er_2O_3 under 377nm excitation

3.5. Upconversion Photo-luminescence Under 980 nm Excitation :

Up-conversion photo-luminescence spectra of Erbium ions doped TZWE glasses (obtained at λexc = 980 nm) in the 500–700 nm spectral range are displayed in Fig. 4. For every glass under study, the peak positions of every recorded emission band essentially stayed the same. Erbium ions ions exhibit strong red and green emission peaks at 668 nm ($^4F_{9/2} \rightarrow {}^4I_{15/2}$) and 548 nm ($^4S_{3/2} \rightarrow {}^4I_{15/2}$)[18,19]. Both of these bands are shown to increase as the concentration of Er^2O^3 is raised from 0.5 mol% to 1.5 mol%, although their strength appears to decrease beyond this concentration. Energy mobility among the Erbium ions may be the cause of an increase in up-conversion photo-luminescence intensity as the mole share of Er_2O_3 rises[20].

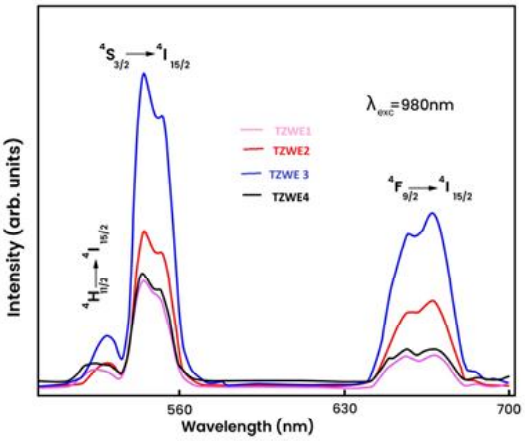

Fig. 4, TZWE glaases with Er_2O_3 under 980nm excitation

3.6. Energy Transfer Mechanism :

Using a simplified energy level diagram from fig. 5, the potential energy transfer pathways for different Erbium ion emission bands are addressed below.

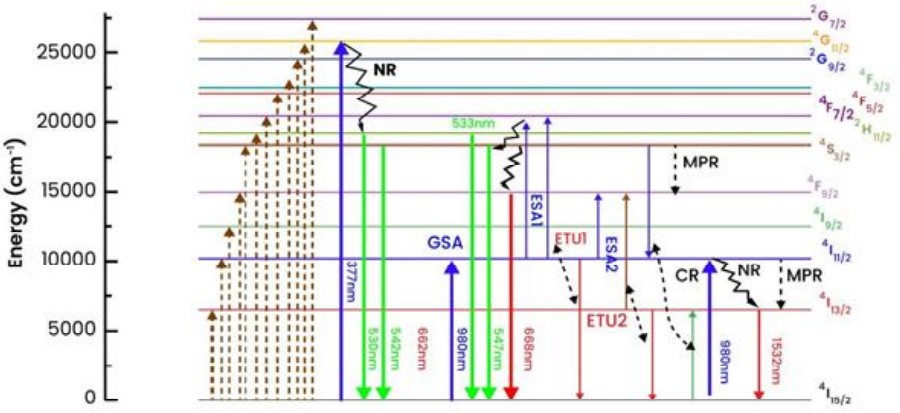

Fig. 5, simplified energy level diagram of Erbium ions in TZWE glass

3.6.1. Photo-luminecence Under 377 nm Excitation :

First, Erbium ions are excited from a $^4I_{15/2}$ ground state to the maximum excited state, $^4G_{11/2}$, under 377 nm laser illumination. Through a non-radiative relaxation mechanism, Erbium ions relaxed from this excited state to the $^2H_{11/2}$ state. The ions of Erbium (in the $^2H_{11/2}$ state) depopulate from the $^2H_{11/2}$ level and move to the $^4S_{3/2}$ level because of the very tiny energy difference (711 cm^{-1})[21] between the two states. Erbium ions released a green emission as they relaxed to ground state at this level. The $^4I_{9/2} \rightarrow {}^4I_{15/2}$ transition also makes the red emission conceivable.

3.6.2. Upconversion Emission mechanism :

Ground-state absorption (GSA) stimulates the Erbium ions in ground state $^4I_{15/2}$ to a higher $^4I_{11/2}$ state at 980 nm excitation. Excited State Absorption (ESA1) is the process by which ions in the $^4I_{11/2}$ excited state are reabsorbed as a photon. The Energy Transfer Upconversion (ETU1) mechanism causes the ions at $^4I_{11/2}$ to depopulate into a higher state, $^4F_{7/2}$. A decreased energy gap causes the Erbium ions at the $^4F_{7/2}$ level to be simultaneously de-excited to $^2I_{11/2}$ and $^4S_{3/2}$ states, after which they relax to a lower ground state with green emission. Additionally, a multiphonon relaxation phenomena causes certain ions from the $^4I_{11/2}$ state to decay to the enduring $^4I_{13/2}$ metastable state. After further absorbing a photon through Excited-State Absorption (ESA2), the ions in the $^4I_{13/2}$ level populate the $^4F_{9/2}$ state through the Energy Transfer Upconversion (ETU2) process. Strong red luminescence is then released as $^4F_{9/2}$ ions are quickly relaxed toward ground state. There is a cross-relaxation energy transfer mechanism[22] with $^4S_{3/2} + {}^4I_{15/2} \rightarrow {}^4I_{13/2} + {}^4I_{15/2}$ between Erbium ions as a result of the intensity of green up-conversion increasing and decreasing with the concentration of Erbium ions.

4. Conclusion

In this work, the optical absorption and upconversion luminescence characteristics of Er^{3+} ion co-doped quaternary tellurite (TZWE) glasses were systematically studied. The results demonstrate that increasing Er_2O_3 concentration leads to a decrease in optical band gap energy and a corresponding increase in refractive index, indicating modifications in the glass network structure and increased polarizability. UV-Vis-NIR absorption spectra confirmed characteristic transitions of Er^{3+} ions, with absorption intensities growing with dopant content. Upconversion photoluminescence under both 377 nm and 980 nm excitation showed prominent green and red emissions, with emission intensity dependent on Er^{3+} concentration. The observed luminescence behavior was explained using energy transfer mechanisms including ground state absorption (GSA), excited state absorption (ESA), and energy transfer upconversion (ETU). Optimal upconversion intensity was observed at moderate Er^{3+} concentrations, beyond which concentration quenching effects were evident. These findings confirm that Er^{3+}-doped tellurite glasses are promising candidates for photonic applications such as solid-state lasers, optical amplifiers, and infrared-to-visible upconversion devices.

References

1. M. Pal, B. Roy, M. Pal, Journal of Modern Physics. *2,* 1062-1066 (2011).
2. D. Muresan, M. Dragan Bularda, C. Popa, L. Baia, S. Simon, Rom. Journ. Phys. *51,* 231-237 (2006).
3. B. Mysen, Eur. J. Mineral. *15,* 781-802 (2003).
4. M.R. Dousti, R.J. Amjad, M.R. Sahar, Z.M. Zabidi, A.N. Alias, A.S.S. de Camargo, Journal of Non-Crystalline Solids. *429,* 70-78 (2015).
5. M. Venkateswarlu, Sk. Mahamuda, K. Swapna, A. Srinivasa Rao, A. Mohan Babu, Suman Shakya, *et al.,* Journal of Luminescence. LUMIN13884 (2016).
6. J. Massera, Nucleation and Growth Behavior of Tellurite-Based Glasses Suitable for MidInfrared Applications, Thesis, Clemson University, 2009.
7. R. K. Sharma , S.K. Mahajan , Z.K. Ansari , G. F. Ansari, Materials Today: Proceedings,https://doi.org/10.1016/j.matpr.2021.09.086
8. Y. Qi, Y. Zhou, L. Wu, F. Yng, S. Peng, S. Zheng, Materials Letters. *125,* 56-58 (2014).
9. R.K. Ramamoorthy, A.K. Bhatnagar, F. Rocca, G. Dalba, M. Mattarelli, M. Montagna, Journal of NonCrystalline Solids *383,* 153-156 (2014).
10. M.K. Halimah, W.M. Daud, H.A.A. Sidek, A.W. Zaidan, A.S. Zainal, Optical properties of ternary tellurite glasses, Materials Science-Poland. *28,* 173-180 (2010).
11. S Jat, RK Sharma, SK Mahajan, M Ashiq, GF Ansari - Materials Today: Proceedings, 2021, Volume 42, Part 2, 2021, Pages 1329-1332.
12. Y. Ding, S. Jiang, B. Hwang, T. Luo, N. Peyghambarian, Y. Himei, *et al.,* Optical Materials. *15,* 123-130 (2000).
13. R. El-Mallawany, R.D. Abdalla, I.A. Ahmed, Materials Chemistry and Physics. *109,* 291-296 (2008).
14. L.M.S. El-Deen, M.Sm Al Salhi, M.M. Elkholy, Journal of Alloy and Compounds. *465,* 333-339 (2008).
15. G. F. Ansari, S. Bairagi, K.S. Bartwal, S.K. Dhiman, S.K. Mahajan Mater. Today: Proc. 80 (Part 2), 427-433.
16. C.H. Basavapoornima, K. Linganna, C.R. Kesavulu, S. Ju, B.H. Kim, W.-T. Han, C.K. Jayasankar, J. Alloy. Comp. 699, 959–968 (2017).
17. Sk Nayab Rasool, B.C. Jamalaiah, K. Suresh, L. Rama Moorthy, C.K. Jayasankar, J. Mol. Struct. 1130, 837–843 (2017).
18. I. Jlassi, H. Fares, H. Elhouichet, J. Lumin. *194,* 569–578 (2018).
19. L. Vijayalakshmi, K. Naveen Kumar, K. Srinivasa Rao, P. Hwang, J. Mol. Struct. 1155, 394–402 (2018).
20. V. Lavín, I.R. Martin, U.R. Rodríguez-Mendoza, V.D. Rodríguez, J. Phys. Condens. Matter *11,* 8739 (1999).
21. P. Babu, H.J. Seo, K.H. Jang, K. Upendra Kumar, C.K. Jayasankar, Chem. Phys. Lett. *445,* 162–166 (2007).
22. C.R. Kesavulu, V.B. Sreedhar, C.K. Jayasankar, K. Jang, D.-S. Shin, S.S. Yi, Mater. Res. Bull. *51,* 336–344 (2014).
23. D.V. Krishna Reddy, T. Sambasiva Rao, S.K. Taherunnisa, A. Suchocki, Y. A. Zhydachevskyy, M. Piasecki, M. Rami Reddy, J. Non-Cryst. Solids *513,* 167–182 (2019).